Optical Engineering 48(3), 033604 (March 2009)

High dynamic range scanning technique

Song Zhang, MEMBER SPIE
Iowa State University
Department of Mechanical Engineering
Virtual Reality Applications Center
Human Computer Interaction
Ames, Iowa 50011
E-mail: song@iastate.edu

Shing-Tung Yau
Harvard University
Department of Mathematics
Cambridge, Massachusetts 02138

Abstract. Measuring objects with a high variation range of surface reflectivity is challenging for any optical method: This paper addresses a high dynamic range scanning technique that can measure this type of object. It takes advantage of one merit of a phase-shifting algorithm: pixel-by-pixel phase retrieval. For each measurement, a sequence of fringe images with different exposures are taken: the brightest ones have good fringe quality in the darkest areas while the darkest ones have good fringe quality in the brightest areas. They are arranged from brighter to darker (i.e., from higher exposure to lower exposure). The final fringe images, used for phase retrieval, are produced pixel-by-pixel by choosing the brightest but unsaturated corresponding pixel from one exposure. A phase-shifting algorithm is employed to compute the phase, which can be further converted to coordinates. Our experiments demonstrate that the proposed technique can successfully measure objects with high dynamic range of surface reflectivity variation. © *2009 Society of Photo-Optical Instrumentation Engineers.* [DOI: 10.1117/1.3099720]

Subject terms: shiny surface; specular surface; three-dimensional measurement; range scanning; phase-shifting; high-dynamic range; Moiré.

Paper 080605RR received Aug. 1, 2008; revised manuscript received Jan. 15, 2009; accepted for publication Jan. 26, 2009; published online Mar. 19, 2009. This paper is a revision of a paper presented at the SPIE conference on Two- and Three-Dimensional Methods for Inspection and Metrology VI, August 2008, San Diego, California. The paper presented there appears (unrefereed) in SPIE Proceedings Vol. 7066.

1 Introduction

Measuring objects with large surface reflectivity variations, such as shiny objects or objects with high contrast, is crucial for diverse applications including manufacturing, biomedical imaging, and entertainment. However, because the optical signal cannot be properly retrieved, it is usually very difficult for an optical method to accurately measure this type of object.

Acquiring three-dimensional (3-D) information of objects is very important. In general, 3-D shape measurement techniques can be classified into two categories: surface contact and surface noncontact. Coordinate measuring machine (CMM) is a typical system that uses surface contact methods for 3-D shape measurement. CMM can almost accurately measure any type of "hard" objects with various scales. Because of its surface-contact measurement nature, this technique is not sensitive to the surface optical properties. However, because it requires surface contact, it is difficult for this technique to measure soft objects. Moreover, because it is a point-by-point measurement technique, its speed is usually very slow.

In contrast, the surface noncontact 3-D shape measurement methods can be used to measure soft objects. Among them, different optical methods are extensively adopted. The optical methods include laser range scanning, stereo vision, Moiré, and structured light methods. Although they have many advantages over CMM, the optical methods suffer if the surface does not have good optical properties. A typical optical method requires the surface to be diffuse and have low reflectivity variations from point to point. Therefore, if the object surface is specular (shiny) or has a very large reflectivity variation range, it is very challenging for any optical method to perform the measurement.

A variety of optical 3-D shape measurement methods have been proposed to deal with shiny surfaces.[1–3] All these proposed methods can alleviate the problems due to surface specular properties to a various degree. However, the method introduced in Ref. 1 uses polarizing filters, which drastically reduces the output light intensity of the projector and the incoming light of the camera, which makes it difficult to measure darker objects. The method proposed by Hu et al.[2] requires repositioning the scanner and finding the corresponding specular areas on the projected fringe image, which usually involves a complicated time-consuming procedure. Moreover, this method also involves a difficult and complicated registration issue for the area measured from different viewing angles. The template-based approach that uses feature extraction[3] suffers if the object does not have strong texture features or the features are too complicated to track. On the other hand, shiny surfaces typically have good optical properties across the surfaces, thus are relatively easier to measure. However, for objects with very high dynamic range of surface reflectivity, all these proposed methods will be potentially problematic.

This paper addresses a high dynamic range scanning (HDRS) technique to measure this type of object. Here, *high dynamic range* means an object surface with a large surface reflectivity variation range, and *range scanning* is another terminology for 3-D shape measurement. Therefore, the HDRS technique is a method that can measure objects with a large surface reflectivity variation range.

This method takes advantage of one merit of a phase-shifting algorithm: pixel-by-pixel phase retrieval. For each measurement, multiple shots of fringe images with different exposures are taken. Therefore, a sequence of fringe images with different overall brightness are captured: the brightest fringe images have good fringe quality in darkest areas, although the brightest areas might be saturated; and the darkest ones have good fringe quality in brightest areas, albeit the fringes in the darker area may be invisible. The sequence of fringe images is arranged from bright to dark (i.e., from higher exposure to lower exposure). The final fringe images, used for phase retrieval, are produced pixel-by-pixel by choosing the brightest but unsaturated corresponding pixel from one shot. A phase-shifting algorithm is employed to compute the phase that can be further converted to 3-D coordinates.

The proposed method was implemented and tested in our previously developed 3-D shape measurement system based on a digital fringe projection and phase-shifting method. Because this method does not require the change of the relative position between the system and the object, the measurement can be done rapidly, and the computation cost does not increase dramatically. Moreover, because this method only requires taking more images with different exposures, it does not increase the hardware cost. The exposure time can be controlled by changing the exposure time of the camera or by adjusting the aperture of the camera lens. Our experiments demonstrate that the proposed technique can successfully measure objects with high dynamic range of surface properties. The same approach can also be used to measure shiny/specular objects because these objects also have larger surface reflectivity variations.

It should be noted that this proposed technique is not limited to 3-D shape measurement systems based on a digital fringe projection and phase-shifting method. The same technique is applicable to any optical measurement techniques that are performed point by point without accessing the neighboring pixel information, such as the Moiré method, laser interferometries, etc.

Section 2 explains the principles of the proposed method. Section 3 describes the hardware system. Section 4 shows some experimental results. Section 5 discusses the advantages and the disadvantages of the proposed approach, and Section 6 summarizes the paper.

2 Principle

Phase-shifting algorithms are widely adopted in optical metrology due to its measurement speed and nonsurface-contact nature.[4] Over the years, numerous phase-shifting algorithms have been developed, including three step, four step, double three step, etc. Different phase-shifting algorithms are developed for different purposes. For example, the three-step algorithm is the simplest one that requires the minimum number of fringe images for 3-D shape measurement; therefore, it is very suitable for rapid 3-D shape measurement purposes. Phase-shifting algorithms have many advantageous features, including being (*i*) less sensitive to local surface reflectivity variations, (*ii*) point-by-point phase retrieval, and (*iii*) less sensitive to ambient light. This proposed method takes full advantage of the merit of retrieving the phase value of different pixels from different shots of fringe images. Therefore, for phase computation, the saturated pixels in a higher exposure are replaced by the corresponding pixels in a lower exposure, while the rest of pixels remain unaltered. This section will explain the details about the proposed technique.

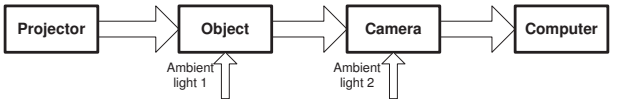

Fig. 1 Procedures of fringe image formation.

2.1 *Three-Step Phase-Shifting Algorithm*

In this research, a three-step phase-shifting algorithm is used for its measurement. The fringe image intensities with a phase shift of $2\pi/3$ are written as

$$I_1(x,y) = I'(x,y) + I''(x,y)\cos[\phi(x,y) - 2\pi/3], \tag{1}$$

$$I_2(x,y) = I'(x,y) + I''(x,y)\cos[\phi(x,y)], \tag{2}$$

$$I_3(x,y) = I'(x,y) + I''(x,y)\cos[\phi(x,y) + 2\pi/3], \tag{3}$$

where $I'(x,y)$ is the average intensity, $I''(x,y)$ the intensity modulation, and $\phi(x,y)$ the phase to be solved for. Solving Eqs. (1)–(3) simultaneously, we can obtain the phase $\phi(x,y)$,

$$\phi(x,y) = \tan^{-1}\left[\frac{\sqrt{3}(I_1 - I_3)}{2I_2 - I_1 - I_3}\right], \tag{4}$$

and the data modulation $\gamma(x,y)$,

$$\gamma(x,y) = \frac{\sqrt{3(I_1 - I_3)^2 + (2I_2 - I_1 - I_3)^2}}{I_1 + I_2 + I_3}, \tag{5}$$

where $\gamma(x,y)$ is the data modulation, which indicates the quality of the point, with 1 being the best. The 3-D information is carried on by the phase $\phi(x,y)$. The value of the phase $\phi(x,y)$ obtained from Eq. (4) ranges from $-\pi$ to $+\pi$. If multiple fringes are used, a phase-unwrapping algorithm[5] is required to remove 2π discontinuities and to obtain a continuous phase map. The unwrapped phase map is further converted to 3-D coordinates if the system is calibrated.[6]

2.2 *Fringe Image Analysis*

For objects with a large range of surface reflectivity (r) variations, some points have very low reflectivity values, $r \to 0$, while other points have large values, $r \to \infty$, such as shiny areas. For the 3-D shape measurement system using a digital fringe projection and phase-shifting method, the captured fringe images are formed through the following procedures (as shown in Fig. 1):

1. Fringe projection. The computer-generated fringe images are projected through a projector onto the object. The output light is the projected fringe images by the projector.

2. Fringe reflection. The projected fringe images are distorted and reflected by the object, point by point. The reflected light includes light from the projector as well as the ambient light 1, $a_1(x,y)$.
3. Fringe acquisition. The camera captures the distorted fringe images, point by point. The captured light includes the light reflected by the object as well as the ambient light 2, $a_2(x,y)$ entering directly into the camera.

Assume a projected fringe image is

$$I^p(x,y) = b + a\cos(x,y).$$

The image is reflected by the object with reflectivity of $r(x,y)$ and the ambient light of $a_1(x,y)$, the reflected image therefore has intensity of

$$I^o(x,y) = r(x,y)[b + a\cos(x,y) + a_1(x,y)].$$

The reflected image is then captured by the camera. Assume the ambient light entering directly to the camera is $a_2(x,y)$ and the camera sensitivity is α. The fringe image actually captured by the camera is

$$I(x,y) = \alpha\{r(x,y)[b + a\cos(x,y) + a_1(x,y)] + a_2(x,y)\}. \quad (6)$$

Thus, the intensity modulation is

$$I''(x,y) = \alpha r(x,y)a, \quad (7)$$

the average intensity is

$$I'(x,y) = \alpha r(x,y)[a_1(x,y) + b] + \alpha a_2(x,y), \quad (8)$$

and the data modulation is

$$\gamma(x,y) = \frac{I''(x,y)}{I'(x,y)} = \frac{r(x,y)a}{r(x,y)[a_1(x,y) + b] + a_2(x,y)}. \quad (9)$$

From Eq. (7), if the surface reflectivity is small [i.e., $r(x,y)$ is small] in order to obtain large intensity modulation value, $I''(x,y)$, camera sensitivity, α, has to be a large. That is, to obtain brighter fringe images, it can increase the exposure time or aperture. However, the quality of data is determined by the intensity modulation $\gamma(x,y)$. To achieve high-quality measurement, $\gamma(x,y)$ must be close to 1. From Eq. (9), to have good fringe contrast, the ambient light, $a_2(x,y)$, entering directly into the camera has to be negligible. If reflectivity value is large [i.e., $r(x,y)$ is sufficiently large] and $a_2(x,y)$ is relatively small, then $a_2(x,y)$ can be neglected. This is the case for shiny objects: $r(x,y)$ is always large. Therefore, to measure a shiny object, only adjusting camera sensitivity is necessary. However, for very small value of $r(x,y)$, ambient light will play an important role, where the measurement environment requires it to be *dark* to eliminate the effect of ambient light.

2.3 *Multiexposure Principle*

For any phase-shifting algorithms, to obtain 3-D data with high quality, the acquired fringe images must have good quality of fringes: larger signal-to-noise ratio (SNR). From the analysis in Section 2.2, for an object with high surface reflectivity [i.e., large $r(x,y)$] and small range of variations, it is very easy to be measured with high quality. However, it is very challenging to measure an object with some areas having very low surface reflectivity and some areas having very high surface reflectivity. This section will explain this novel HDRS technique that uses a multiexposure method.

For the multiexposure technique, a sequence of fringe images [$I_k^n(x,y)$, with $k=1,2,3$ and $n=1,2,3,\ldots,N$] are acquired for the measurement. For each set n, three fringe images with a phase shift of $2\pi/3$ are captured under the same exposure. In other words, each set of fringe images can be used to independently reconstruct a 3-D shape for good points. Assume the brightness of the fringe image sets decreases from one exposure to the next, i.e.,

$$I_k^n(x,y) > = I_k^{(n+1)}(x,y),$$

then the final fringe images used for 3-D measurement are

$$I_k^f(x,y) = I_k^m(x,y), \quad m = \min(n), \quad (10)$$

with $I_1^m < 255$, $I_2^m < 255$, and $I_3^m < 255$, while $I_1^{m-1} \geqslant 255$, or $I_2^{m-1} \geqslant 255$, or $I_3^{m-1} \geqslant 255$. Here, $m=\min(n)$ is the minimum function of n. That is, each pixel of the fringe images is generated by selecting the brightest but unsaturated corresponding pixel from one set of fringe images, namely,

$$I_1^f(x,y) = \max\{I_1^n(x,y) | I_1(x,y) < 255, I_2(x,y) < 255, I_3(x,y) < 255\}, \quad (11)$$

$$I_2^f(x,y) = \max\{I_2^n(x,y) | I_1(x,y) < 255, I_2(x,y) < 255, I_3(x,y) < 255\}, \quad (12)$$

$$I_3^f(x,y) = \max\{I_3^n(x,y) | I_1(x,y) < 255, I_2(x,y) < 255, I_3(x,y) < 255\}. \quad (13)$$

Figure 2 illustrates how to form the final fringe images pixel by pixel. For an arbitrary point on the image, its intensity values of three fringe images use the exposure m, so that all intensity values of this pixel are not saturated while the same pixel of the previous set of images with higher exposure is saturated for at least one fringe image.

Because the phase-shifting algorithm computes the phase point by point, the fringe images obtained in Eq. (10) can be substituted into Eq. (4) to obtain the phase pixel by pixel that can be further converted into 3-D coordinates.

3 System Setup

In this research, we developed a 3-D shape measurement system based on a digital fringe projection and phase-shifting method. As shown in Fig. 3, a computer graphics card sends fringe image signals to a digital-light-processing (DLP) projector that projects them onto the object. The fringe images were reflected and sensed by a charge-coupled device camera that were further converted to digital images by a frame grabber. In this research, the DLP projector used is PLUS U5-632h with a resolution of 1024×768, the camera is Jai Pulnix TM-6740CL with a resolution of 640×480 at a frame rate up to 200 fps the camera lens is Fujinon HF25SA-1 with a focal length of

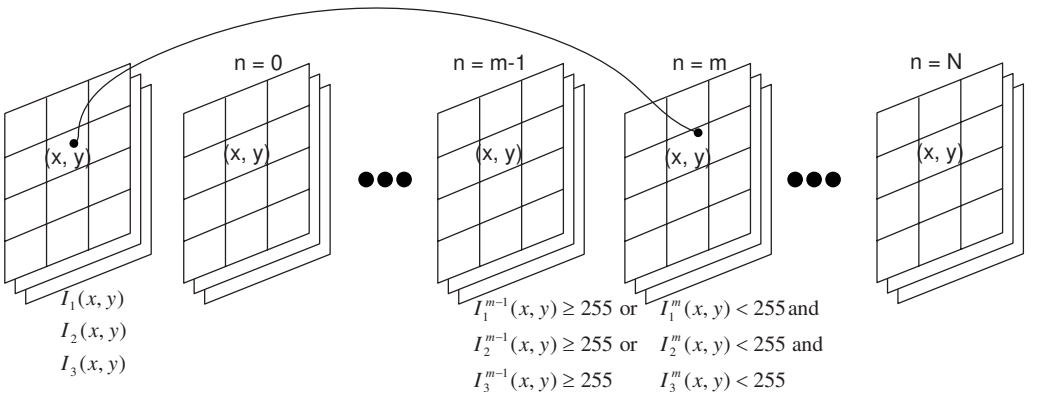

Fig. 2 Formation of each fringe image pixel from a sequence of fringe images with different exposures.

25 mm, and the frame grabber is Matrox Solios XCL that has a camera-link interface. The digital fringe images acquired by the camera are then processed to retrieve the phase using a phase-shifting algorithm. The phase is further converted to 3-D coordinates using the calibrated system parameters. The system was calibrated using our previously proposed method.[6]

4 Experiments

To verify the performance of the system, we measured a black-and-white (B/W) checkerboard using the hardware system addressed in Section 3. The B/W checkerboard with pure black and white squares was printed using a B/W laser printer onto a fine paper, and then was glued onto a flat surface (a piece of glass). Figure 4(a) shows the B/W checkerboard. It is obvious that such a checkerboard is very difficult to measure with a single exposure because the contrast between the black and white squares is very large, albeit its surface is diffuse. Figure 4(b) shows that when the white squares have good fringes, the fringes on those black ones are almost invisible. Figure 4(c) shows that the black checkers have good fringes while the white squares are saturated. Hence, neither exposure is sufficient to correctly measure the whole surface. On the other hand, if the white areas use fringe pixels as shown in Fig. 4(b) and black areas use fringe pixels in Fig. 4(c). The whole surface can be measured. Figure 4(d) shows the resultant fringe images by taking the better pixels from Fig. 4(b) and 4(c).

Figure 5 shows the 3-D measurement result. Figures 5(a)–5(c) shows three fringe images by combining these two exposures. Figures 5(d) shows the wrapped phase map. Although the fringe images are not seemingly regular, the phase map is very normal. Figure 5(e) shows the measurement result rendered in 3-D shaded mode, while Fig. 5(f) shows the measurement result with texture mapping. It can be seen here that the checkerboard squares are still clearly seen, but the geometry is well captured. Figure 5(g) shows one cross section of the measurement. Figure 5 shows that between the boundary of the black and white squares, the noises are significantly larger. It is not clear to us the true cause of this problem: it might be induced by the sampling of the camera in these transition areas. This example demonstrated that the proposed approach is able to measure a high-contrast object with two exposures.

Moreover, we measured a more complex object, a China vase. It has high dynamic range of surface reflectivity variations. Figure 6 shows the fringe image acquisition process. Figure 6(a) shows the color photograph of the measured object taken by a digital camera. Unlike the checkerboard shown in the previous example, this object has larger surface reflectivity variation range; thus, two exposures are

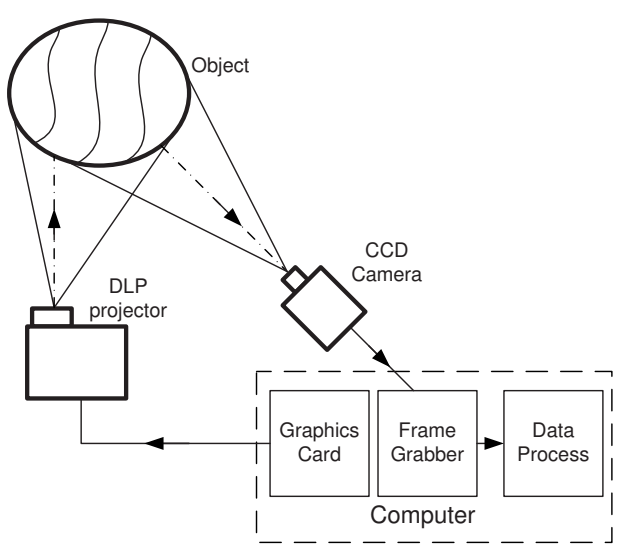

Fig. 3 System setup.

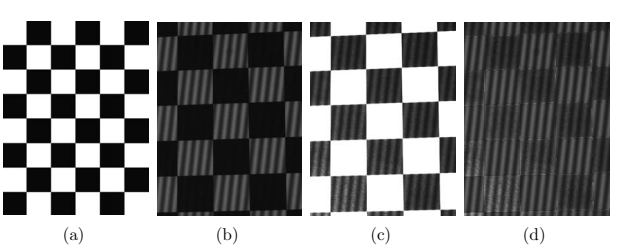

Fig. 4 Fringe image formation of the checkerboard object: (a) B/W checker-board, (b) one fringe image with the white squares well illuminated, (c) one fringe image with the black squares well illuminated, and (d) combined fringe image by taking better pixels from (b) and (c).

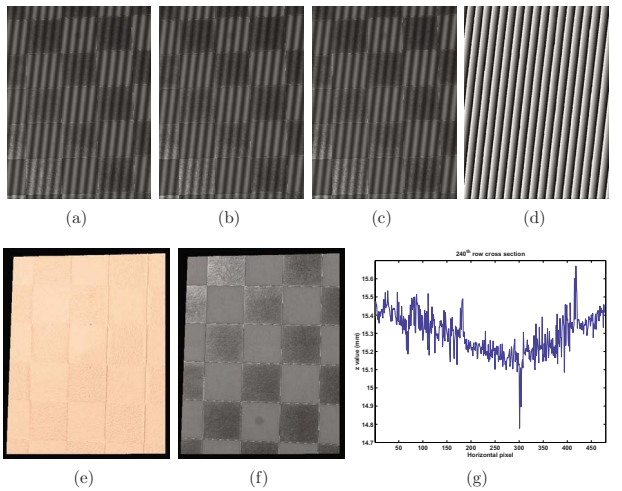

Fig. 5 Experimental results of a shining object. (a–c) Three fringe images with a phase shift of $2\pi/3$, (d) the wrapped phase, (e) 3-D reconstructed result rendered in shaded mode, (f) 3-D result with texture mapping, and (g) cross-section plot of the 320th row.

not sufficient. We used 23 exposures in order to obtain high-quality data. Figure 6(b) shows the fringe image with the longest exposure. Most of the points are saturated thus are not usable for the measurement. Figure 6(c) shows the fringe image points that are eventually used for measurement. The black areas indicate that no good data points are captured yet. After a shorter exposure, we formed the fringe image shown in Fig. 6(d). More good data points are acquired after the second exposure. Figures 6(e) and 6(d) show the resultant fringe images after the exposure 3 and exposure 4, respectively. For this case, 23 exposures are used to obtain good quality. Video 1 shows the final fringe images after each exposure. The left images show the raw

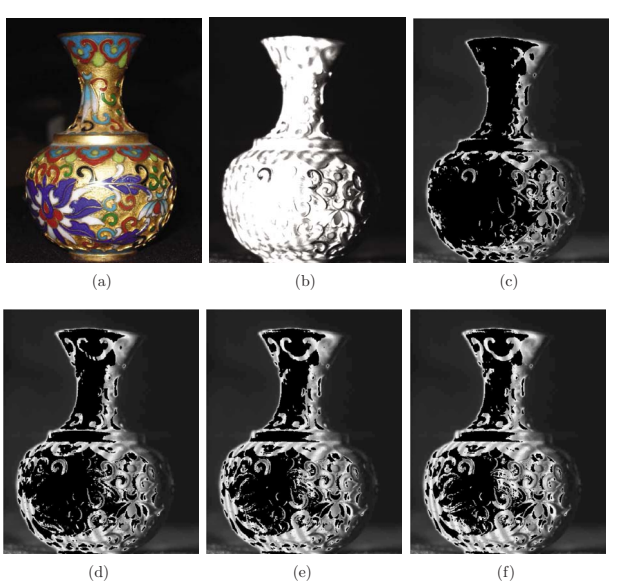

Fig. 6 Experimental results of the vase: (a) Color photograph of the vase, (b) fringe image for exposure 1, (c) fringe image points usable after exposure 1, (d) fringe image points usable after exposure 2, (e) fringe image points usable after exposure 3, and (f) fringe image points usable after exposure 4.

Video 1 Fringe image-acquisition process using multiple exposures (QuickTime, 1.2 MB). [URL: http://dx.doi.org/10.1117/1.3099720.1].

fringe image for each exposure, and the right images show the resultant fringe image after applying the propose method.

Figure 7 shows the measurement result of the vase. Figure 7(a) shows one of the final fringe images. Figure 7(b) shows the wrapped phase map, and Fig. 7(c) shows the mask used to remove the background. Figures 7(e) and 7(f) show the 3-D result rendered in different modes. It can be seen that the small size of rings (1 mm width) are well captured and the details of the objects are properly measured. It should be noted that the results shown in Fig. 7 are all smoothed by a 3×3 Gaussian filter to remove the most significant random noises. Video 2 shows the measurement result from different viewing angles and different zooms.

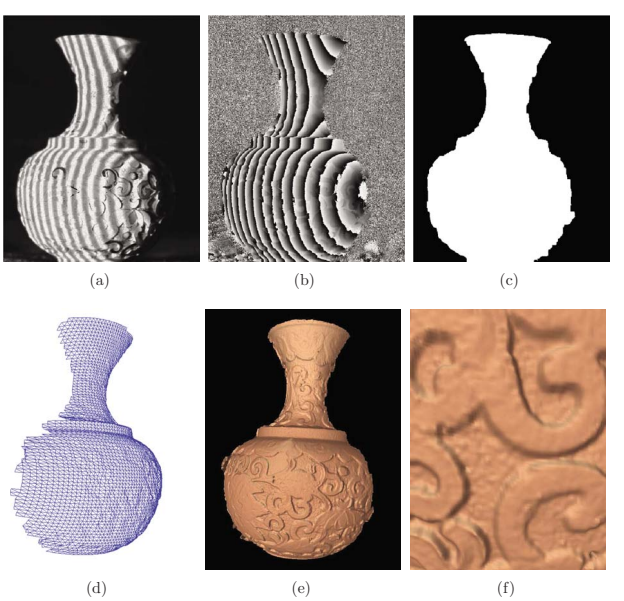

Fig. 7 Measurement result of the vase (size of the vase is ~75 mm in height and 50 mm in width): (a) One final phase-shifted fringe images, (b) the wrapped phase map, (c) the mask used to remove the background, (d) rendered in wireframe mode, (e) rendered in shaded mode, the details of the vase rings are well captured, and (f) zoom-in view of a mall region (ring width is ~1 mm).

Video 2 Measurement result of the vase shown in a video (QuickTime, 1.25 MB). [URL: http://dx.doi.org/10.1117/1.3099720.2].

This experiment demonstrated that the proposed method can successfully measure objects with large dynamic surface reflectivity.

5 Discussion

From the experimental results shown previously, it can be seen that the advantages of the proposed method are obvious:

1. Low cost. This method does not requires the use of additional hardware. It only needs to adjust the exposure of the camera. Therefore, no additional cost of the hardware is necessary.
2. Simple. The whole area can be measured once without changing the relative position of the object and the system; hence, no sophisticated registration and merging algorithms are required.
3. Fast. In our simple example of the checkerboard, only two exposures are needed. For an object with a significantly large dynamic range of surface reflectivity variations, more exposures are needed to measure every level of the reflectivity areas. For the vase example, 23 exposures are need. However, because all the operations can be done auto-matically, adjusting the aperture or controlling the exposure time, the measurement can be done rapidly.
4. Generic. The proposed method theoretically works for any surface reflectivity variations. The larger dynamic range the object has, the more exposures needed. Of course, the more exposure used, the better the result will be, although the slower the measurement process.

In the meantime, because a phase-shifting algorithm is less sensitive to the ambient light, it is less sensitive to local surface reflectivity variations. Therefore, the phase-shifting algorithm is robust to measure objects with a certain range of surface reflectivity variations. However, for large surface reflectivity variations, the SNR is very small for low-reflectivity areas, the quality of measurement is hard to be ensured, where the ambient light requires it to be controlled at a very low level. Therefore, theoretically, the proposed method can be used to measure any object with any dynamic range of surface reflectivity variations provided that there is no ambient light.

From our previous discussions, the only requirement for the success of this proposed technique is point-by-point measurement. Therefore, any optical methods that satisfy this condition can implement this proposed technique for the measuring surface with large reflectivity variations, which include Morié, laser interferometries, etc.

6 Conclusion

In summary, this paper has presented a novel method to measure object with large range of surface reflectivity variations. It utilizes a multiexposure, phase-shifting–based method. For this method, a sequence of fringe images with different exposures are taken. For each exposure, a number of phase-shifted fringe images, required to retrieve the phase, are taken. We changed the exposure by adjusting the aperture of the camera lens, which is similar to controlling the exposure time of the camera. The brightness of the fringe images ranges from bright to dark; thus, the brightest fringe images are overall well illuminated although a large area of pixels are saturated. On the contrary, the darkest fringe images do not have any pixels saturated although most of areas of the fringes might not be visible. The final fringe images, used for 3-D reconstruction, are formed by choosing the brightest but unsaturated corresponding pixel from the fringe-image sequence. For this method, the saturated pixels in the higher exposure are replaced by the corresponding pixels of the lower exposures. Therefore, properly measuring the bright area does not affect the rest areas. We implemented the proposed method into a 3-D shape measurement system. Our experiments verified that the proposed method can be used to measure the objects with high surface reflectivity variations. It should be noted that a three-step phase-shifting algorithm is used for this research, but the proposed method is not limited to this phase-shifting algorithm.

Acknowledgments

We thank Brandon Bodnar for his grammatical assistance with the paper.

References

1. Y. Yoshinori, M. Hiroyuki, N. Osamu, and I. Tetsuo, "Shape measurement of glossy objects by range finder with polarization optical system," *Gazo Denshi Gakkai Kenkyukai Koen Yoko* **200**, 43–50 (2003) [in Japanese].
2. Q. Hu, K. G. Harding, X. Du, and D. Hamilton, "Shiny parts measurement using color separation," *Proc. SPIE* **6000**, 6000D1–8 (2005).
3. R. Kokku and G. Brooksby, "Improving 3D surface measurement accuracy on metallic surfaces," *Proc. SPIE* **5856**, 618–624 (2005).
4. D. Malacara, Ed., *Optical Shop Testing*, 3rd ed. (John Wiley and Sons, New York, 2007).
5. S. Zhang, X. Li, and S.-T. Yau, "Multilevel quality-guided phase unwrapping algorithm for real-time three-dimensional shape reconstruction," *Appl. Opt.* **46**, 50–57 (2007).
6. S. Zhang and P. S. Huang, "Novel method for structured light system calibration," *Opt. Eng.* **45**, 083601 (2006).

Song Zhang is an assistant professor of mechanical engineering, at Iowa State University, where he is also a faculty affiliate of the virtual reality applications center and graduate faculty of the human computer-interaction program. He received his PhD in mechanical engineering from Stony Brook University in 2005 and worked as a post-doctor fellow at Harvard University. His major research interests include real-time 3-D optical metrology, 3-D machine and computer vision, and geometry processing.

Shing-Tung Yau is a professor of mathematics at Harvard University. He received his PhD in mathematics from the University of California-Berkeley in 1971. He received a number of awards including the Fields Medal in 1982, a MacArthur Fellowship in 1984, the Crafoord Prize in 1994, and the (U.S.) National Medal of Science in 1997.